ACS Catalysis

Research Article

pubs.acs.org/acscatalysis

Acid Properties of Nanocarbons and Their Application in Oxidative Dehydrogenation

Guodong Wen,[†] Jiangyong Diao,[†,‡] Shuchang Wu,[†] Weimin Yang,[§] Robert Schlögl,[∥] and Dang Sheng Su*[,†]

[†]Shenyang National Laboratory for Materials Science, Institute of Metal Research, Chinese Academy of Sciences, Shenyang 110016, China

[‡]Graduate University of Chinese Academy of Sciences, Beijing 100049, China

[§]Shanghai Research Institute of Petrochemical Technology, 1658 North Pudong Road, Shanghai 201208, China

[∥]Department of Inorganic Chemistry, Fritz Haber Institute of the Max Planck Society, Faradayweg 4-6, Berlin 14195, Germany

Supporting Information

ABSTRACT: Carbon is emerging as an important metal-free catalyst for multiple types of heterogeneous catalysis, including thermocatalysis, photocatalysis, and electrocatalysis. However, the study of mechanisms for carbon catalysis has been impeded at an early stage due to the lack of quantitative research, especially the intrinsic kinetics (e.g., intrinsic TOF). In many carbon-catalyzed reactions, the surface oxygenated groups were found to be the active sites. Recently, we have shown that these oxygenated groups could be identified and quantified via poisoning by small organic molecules; however, these small molecules were toxic. As most of the oxygenated groups are acidic groups, they could also be identified and quantified with respect to the acid properties. More importantly, the method based on acid properties is very green and environmentally benign, because only inorganic bases are added. In this work, the acid properties of carbon nanotubes (CNTs) treated by concentrated HNO_3 were thoroughly studied by mass titration and Boehm titration. The two titration methods were also compared to the conventional methods for acidity analysis including NH_3 pulse adsorption, NH_3-TPD, and FT-IR. Boehm titration was very effective to quantify the carboxylic acid, lactone, phenol, and carbonyl groups, and the findings were consistent with the results from XPS and NH_3 pulse adsorption. These CNTs were applied in the oxidative dehydrogenation (ODH) of ethylbenzene, and the activity of these catalysts exhibited a good linear dependence on the number of carbonyl groups. The value of TOF for the carbonyl group obtained from Boehm titration was 3.2×10^{-4} s^{-1} (245 °C, atmosphere pressure, 2.8 kPa ethylbenzene, 5.3 kPa O_2). For better understanding the acidity of nanocarbon, these CNTs were also applied in two acid-catalyzed reactions (Beckmann rearrangement and ring opening), and a good linear relationship between the conversion and the number of acidic sites was found.

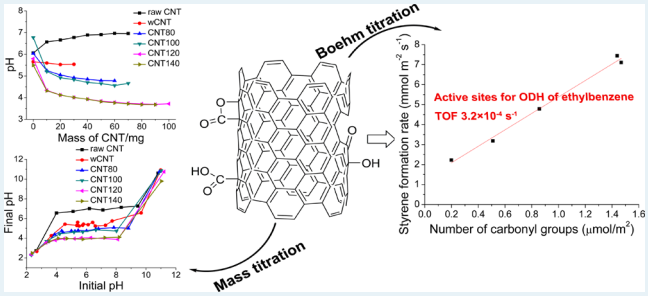

KEYWORDS: *acid properties, nanocarbon, oxidative dehydrogenation, mass titration, Boehm titration*

1. INTRODUCTION

Recently, nanocarbons (e.g., carbon nanotubes, graphene, mesoporous carbon nitride, and nanodiamond) are emerging as important nonmetal catalysts for many types of heterogeneous catalysis, including thermocatalysis (e.g., dehydrogenation of ethylbenzene and alkanes,[1−4] oxidation of alcohol,[5,6] hydrogenation of nitrobenzene,[7] hydrogenation of olefin,[8] and cyclohexane oxidation[9,10]), photocatalysis,[11] and electrocatalysis.[12] These nanocarbon catalysts show significant advantages such as stable structure, high acid/base resistance, tunable surface functional groups, unique electron properties, convenient recycling, and reusability compared to the traditional metal and metal oxide based catalysts.[1,2,13−15] However, the research of mechanisms for nanocarbon catalysts grows slowly due to the complex surface structure, coexistence of various functional groups, residual metal impurities, and so forth.[1,2,16,17] Consequently, an understanding of the detailed catalytic roles of carbon catalysts and the intrinsic kinetic study of these catalysts remain a challenge, because the active sites are difficult to be identified and quantified.

The surface oxygenated groups on the nanocarbon have been found to be very critical in the carbon-catalyzed reactions.[1,2,5,18−23] As most of the oxygenated groups are acidic groups, it is very effective to study them with respect to the acid properties. Besides, the research on the acid properties of the nanocarbon will shed some light on the study of acid properties of the solid acid catalyst, which is one of the most widely applied catalysts in many large-scale industrial processes such as

Received: July 18, 2014
Revised: April 21, 2015
Published: April 30, 2015

ACS Publications © 2015 American Chemical Society

DOI: 10.1021/acscatal.5b00307
ACS Catal. 2015, 5, 3600−3608

catalytic cracking and hydroisomerization. NH_3-TPD is a widely used tool to analyze the surface acid properties of solid acid materials,[24,25] whereas the number of the specific functional groups could not be quantified.

Point of Zero Charge (PZC) is very useful to analyze the surface acidity of nanocarbon materials and characterize the surface oxygenated groups, and it is also very helpful to prepare metal-supported catalysts via the "strong electrostatic adsorption" method.[26,27] The generally used method to analyze the PZC is based on the zeta potential measurement; the initial pH of the solution should be changed during the analysis, and the materials should be well dispersed in the solution, which makes the method very complex and time-consuming, especially for the material that could not be easily dispersed in water (e.g., carbon materials). In contrast, mass titration is considered to be very simple and effective to study the PZC of materials, because it is unnecessary to change the initial pH of the solution and extensively disperse the materials.[28] Although the PZC could effectively describe the overall acid properties of the surface oxygenated groups, these groups could not be quantified. It was reported that four oxygenated groups, including carboxylic acid, lactone, phenol, and carbonyl groups, could be measured via Boehm titration by adding bases with different basicity.[29,30]

Present mechanism research on the carbon catalyst suggests that the ketonic carbonyl groups might be the active sites for ODH of ethylbenzene and light alkanes.[31−33] Zarubina et al. found that nanocarbon catalyst was very active and stable under industrially relevant conditions,[34] suggesting that the nanocarbon catalyst was very promising for industrial application. However, the ODH reactions lack the quantitative research, especially the intrinsic kinetics (e.g., intrinsic TOF). Although XPS and TPD were applied by some researchers to quantify the surface oxygenated groups,[35] there was a controversy about the peak fitting. Besides, it is almost impossible to deconvolute the XPS and TPD spectra into many individual specific groups, as the signals of these groups overlap. Recently, it was shown by our group that the carbonyl, phenol, and carboxylic acid groups could be identified and quantified via poisoning by phenylhydrazine, benzoic anhydride, and 2-bromo-1-phenylethanone, respectively.[36] However, these organic molecules used in that method were toxic. Herein, we show that the oxygenated groups could also be studied with respect to the acid properties. More importantly, this method is green and environmentally benign, because only inorganic bases are added. A series of carbon nanotubes (CNTs) treated by concentrated nitric acid at temperatures in the range of 80 to 140 °C were prepared in this work. The acid properties were studied by mass titration and Boehm titration, which were then compared to the conventional methods for acidity analysis, including NH_3 pulse adsorption, NH_3-TPD, and FT-IR. The activity of these CNTs for ODH of ethylbenzene was investigated, and a good linear relationship was found between the activity and the surface number of carbonyl groups. For better understanding the acidity of the nanocarbon, these CNTs were also applied in two typical acid-catalyzed reactions (Beckmann rearrangement and ring opening).

2. EXPERIMENTAL SECTION

2.1. Materials. Carbon nanotubes (surface area, 215 m^2/g) were obtained from Shandong Dazhan Nano Materials Co., Ltd. (Zouping County, Binzhou City, Shandong Province, China). Ethylbenzene (analytical grade) was bought from Alfa Aesar. Concentrated nitric acid and concentrated hydrochloric acid were supplied by Sinopharm Chemical Reagent Co., Ltd.

2.2. Sample Preparation. Prior to the HNO_3 treatment, the pristine CNTs were washed with concentrated HCl at room temperature for 20 h to remove the residual metal impurities, as nonoxidative acid was reported to be more efficient than oxidative acid (e.g., HNO_3).[37] Then, the sample was washed with distilled water to neutral (denoted as wCNT). After being sonicated in concentrated HNO_3 for 10 min, the CNTs were refluxed at 80, 100, 120, and 140 °C (the temperatures of the oil bath) in concentrated HNO_3 for 2 h, respectively. Samples were then washed with distilled water to neutral, and the obtained samples were referred as CNT80, CNT100, CNT120, and CNT140, respectively. The 20 wt % V_2O_5/MgO catalyst was prepared as follows. $H_2C_2O_4$ was added to an aqueous solution of $Mg(NO_3)_2$ at 70 °C. The resulting MgC_2O_4 was washed with deionized water, dried at 120 °C overnight, and then calcined at 500 °C in air for 8 h to complete the decomposition of MgC_2O_4 to MgO. The obtained MgO powder was added into an aqueous solution of ammonium vanadate at 70 °C, and the solution was evaporated to dryness. Finally, the resulting solid was calcined at 600 °C in air for 6 h.

2.3. Sample Characterization. The XRD patterns of the samples were obtained using a D/MAX-2500 PC X-ray diffractometer with monochromatized Cu Kα radiation (λ = 1.54 Å). Transmission electron microscopy (TEM) images were recorded on a FEI Tecnai T12 with an accelerating voltage of 120 kV. Thermogravimetric analysis (TGA) was performed on a Netzsch-STA 449 F3 instrument in air with 10 °C/min from 35 to 900 °C. The specific surface area was measured by the Brunauer−Emmett−Teller (BET) method using nitrogen adsorption−desorption isotherms on a Micrometrics ASAP 2020 system. Pore size distributions were estimated from the desorption branches of the isotherms using the Barrett−Joyner−Halenda (BJH) method. The total pore volumes (V_P) were estimated on the basis of the number of N_2 molecules adsorbed at a relative pressure of 0.99. The X-ray photoelectron spectroscopy (XPS) spectra were carried out on an ESCALAB 250 XPS system with a monochromatized Al Kα X-ray source (1486.6 eV) with correction for cross sections and escape depths. The data fitting was performed by fixing the peak maximum within ±0.4 eV for all the spectra and applying a full width at half-maximum (fwhm) of 1.2−1.6 eV by means of Avantage analysis software. Raman spectroscopy was tested by a LabRam HR 800 using 633 nm laser. Temperature-programmed desorption (TPD) was performed on Catlab with a QIC-20 gas analysis system from Hiden Analytical in He with 10 °C/min from 150 to 900 °C and kept at this temperature for 20 min. NH_3 pulse adsorption was conducted on the above-mentioned Catlab at 35 °C to analyze the acidity, and all the samples were pretreated at 120 °C in He for 2 h prior to adsorption. After the sample was saturated with NH_3, the NH_3-TPD experiment was conducted in He with 10 °C/min from 35 to 900 °C. The acidity was also measured by pyridine and NH_3 adsorption with FT-IR (Tensor 27, Bruker). First, the samples were evacuated in situ at 120 °C in an IR cell for 1 h. After the temperature decreased to room temperature, the background spectra were recorded. Then pyridine and NH_3 was introduced into the cell, respectively, and the IR spectra were acquired. Finally, the samples were evacuated in situ at room temperature, and then the IR spectra were taken.

2.4. Mass Titration and Boehm Titration. Two methods of mass titrations were performed to determine the Point of

DOI: 10.1021/acscatal.5b00307
ACS Catal. 2015, 5, 3600−3608

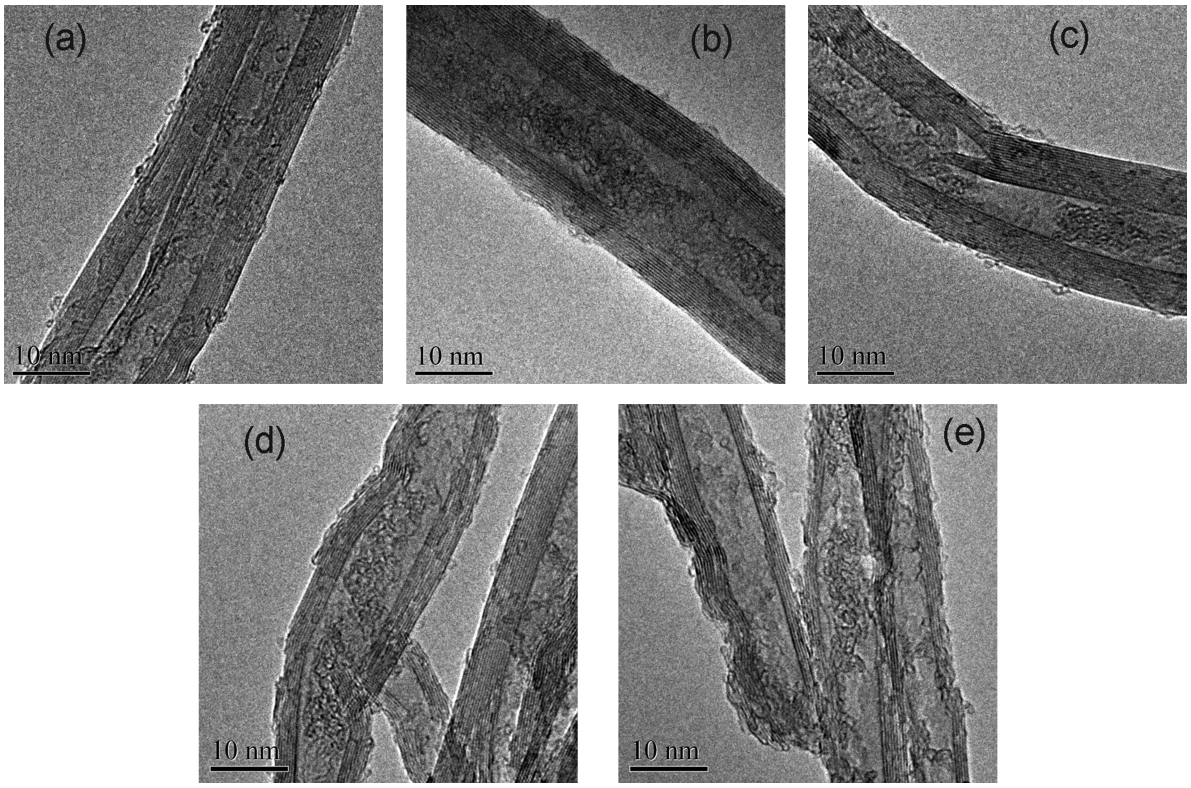

Figure 1. TEM images of (a) wCNT, (b) CNT80, (c) CNT100, (d) CNT120, and (e) CNT140.

Zero Charge (PZC) as follows. For method 1, CNTs sample was added in 10 mg increments into 10 mL of deionized water while stirring. The resulting pH was measured after 10 min to reach an equilibrium pH value. The PZC was determined from the appearance of a plateau in the plot of pH vs mass. As to method 2, 10 mL of a solution with a given initial pH from 2 to 12 was prepared by adjusting with HCl or NaOH. Fifty milligrams of CNTs sample was added and stirred for 30 min to reach an equilibrium pH value. The pH value was then measured, and the PZC was determined from the plateau in the plot of final pH vs initial pH. The carboxylic acid, lactone, phenol, and carbonyl groups were quantified by Boehm titration. Specifically, 0.35 g sample was placed in 35 mL each of the following 0.1 mol/L solutions: $NaHCO_3$, Na_2CO_3, NaOH, and C_2H_5ONa. After slowly stirred for 24 h, 10 mL of each filtrate was pipetted, and the excessive base was titrated with 0.1 mol/L HCl. The number of various types of acid groups was calculated under the assumption that C_2H_5ONa neutralized carboxylic acid, lactone, phenol, and carbonyl groups; NaOH neutralized carboxylic acid, lactone, and phenol groups; Na_2CO_3 neutralized carboxylic acid and lactone groups; $NaHCO_3$ neutralized carboxylic groups.

2.5. Catalytic Test of CNTs. The ODH reactions were carried out on CNTs catalysts (100 mg) in a fixed-bed quartz reactor at atmospheric pressure at various temperatures from 518 to 573 K. Carbon catalysts were fixed between two plugs of quartz wool. Reaction mixtures contained ethylbenzene, oxygen, and helium at a typical gas flow rate of 6000 mL h^{-1} g_{cat}^{-1}, and the flow rates were adjusted to give the desired ethylbenzene and O_2 pressures (2.8 kPa and 1.1−28 kPa, respectively). The products were monitored by an online gas chromatograph (Agilent 7890) with FID and TCD detectors.

The Beckmann rearrangement of cyclohexanone oxime was performed as follows. Cyclohexanone oxime (115 mg) and CNTs catalysts (50 mg) were dispersed in benzonitrile (10 mL) in a flask. The reaction mixture was carried out at 130 °C for 6 h. The products were analyzed by GC (Agilent 7890) with HP-5 column, and DMF (50 μL) was added as a GC internal standard.

The ring opening of styrene oxide with methanol was performed in a flask in the presence of 0.5 mL of styrene oxide and 10 mL of methanol over 50 mg CNTs catalysts at 50 °C for 3 h. The products were analyzed by GC (Agilent 7890) with HP-5 column, and ethylbenzene (200 μL) was added as a GC internal standard.

3. RESULTS AND DISCUSSION

3.1. Catalyst Characterization. The TEM images of wCNT and HNO_3 oxidized CNTs at different temperatures from 80 to 140 °C are shown in Figure 1. It appears that the morphology of the CNTs samples did not significantly change after the treatment in nitric acid. A little more amorphous carbon is observed on the surface of the CNTs treated at higher temperatures. The initial temperature of these CNTs from the TG curves slightly shifts to lower temperatures at the samples with high treatment temperature (Figure S1). The reason can be attributed to the amorphous carbon formed during the refluxing process in nitric acid at high temperatures. The above results indicate that the graphitic structure of the CNTs used in this study was slightly destroyed after treatment in nitric acid, and a small amount of amorphous carbon formed during the nitric acid treatment.

However, from the XRD results, it is found that all these CNTs samples depict typical (002), (100), (004), and (110) graphitic diffraction peaks (Figure S2), indicating that the

DOI: 10.1021/acscatal.5b00307
ACS Catal. 2015, 5, 3600−3608

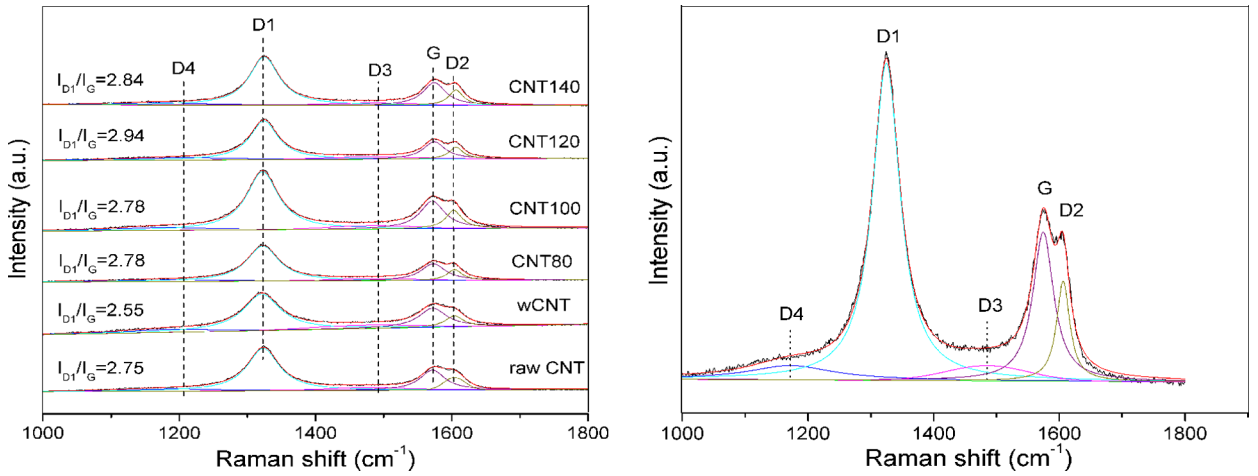

Figure 2. Raman spectra of these CNTs and a typical curve fitting of CNTs sample (CNT140).

graphene layers of these CNTs samples remained almost intact after the treatment in nitric acid. It is also found that the position of these peaks does not obviously shift after the treatment, which demonstrates that the expansion of the lattice that is likely induced by the HNO_3 intercalation during refluxing could be neglected.[38]

Raman spectroscopy is widely used to study the structure of nanocarbon materials.[39,40] The Raman spectra were deconvoluted into four Lorentzian peaks and one Gaussian peak definitely according to Sadezky et. al,[39] and the I_{D1}/I_G values from the Raman spectra of these CNTs were determined by the intensity ratio of the D1 band (~1350 cm^{-1}) and G band (1580 cm^{-1}). As shown in Figure 2, the I_{D1}/I_G values of the CNTs do not obviously change after refluxed in nitric acid, indicating that the ordered structure of the CNTs was not significantly destroyed and that the number of surface defects did not obviously increase after the nitric acid treatment.

The results from N_2 adsorption/desorption analysis show that all the samples exhibit type IV isotherms (Figure S3). The BET surface area of the CNTs with the treatment at low temperatures remained similar (Table 1), however the surface

Table 1. Textural Properties of CNTs

sample	S_{BET} (m^2/g)	S_{micro} (m^2/g)	V_p[a] (cm^3/g)	D_p[b] (nm)
wCNT	233	2	1.60	21.5
CNT80	233	0	1.69	23.0
CNT100	231	2	1.33	18.9
CNT120	250	12	1.34	19.2
CNT140	276	11	1.41	18.3

[a]Pore volume measured at the single point of P/P_0 = 0.99. [b]BJH desorption average pore diameter.

area significantly increased when the treatment temperature increased above 120 °C. All the samples show bimodal pore size distribution (Figure S4), the peaks at small pore width might be from the inner side of the CNTs, while the peaks at large pore width are likely contributed by aggregated pores among the isolated CNTs.

As we all know, HNO_3 treatment is an effective tool to functionalize the carbon materials with oxygenated groups.[1,2,31] These surface oxygenated groups can be detected by XPS analysis, and the O 1s and C 1s spectra are shown in Figure 3 and Figure S5, respectively. The O 1s spectra were

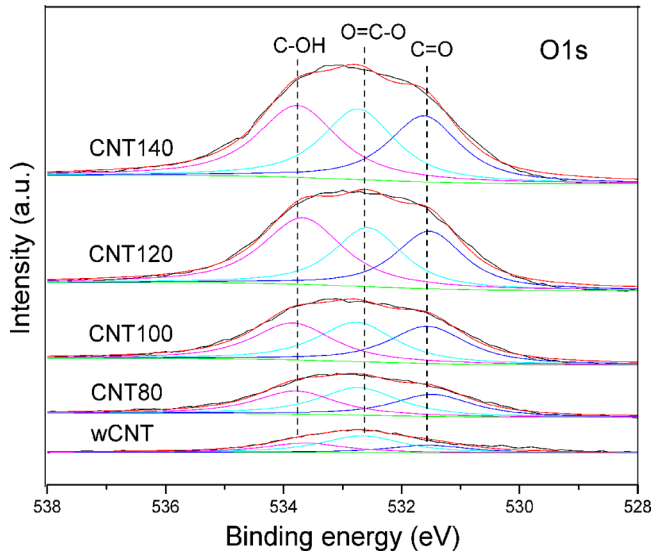

Figure 3. O 1s XPS spectra of these CNTs samples.

deconvoluted into three peaks at 531.4 eV (C═O), 532.5 eV (O═C−O), and 533.7 eV (OH), respectively.[36] As shown in Figure 3, the surface concentration of these oxygen species significantly increases with the increase of treatment temperature. The C 1s peak is not deconvoluted because the deconvolution of C 1s peak is generally more difficult and ambiguous, as the contribution from the C 1s intensity of the carbon in oxygenated groups is very low compared to the whole C 1s signal.[36,41]

The functional oxygen groups can also be identified from the evolution profiles of CO_2 (Figure S6) and CO (Figure S7) during the TPD test. The evolution profiles of CO_2 were deconvoluted into three peaks around 260 °C (carboxylic acid), 400 °C (carboxylic anhydride), and 600−700 °C (lactone).[16,42] Two peaks at around 700 and 870 °C observed from the evolution profiles of CO could be assigned to phenol and carbonyl groups, respectively. It is found that the O content for O═C−O groups (sum of carboxylic acid, carboxylic anhydride, and lactone) and phenolic group from TPD profiles shows nearly linear dependence on the O content for O═C−O groups and phenolic group from XPS spectra (Figure S8 and S9), respectively, indicating that the TPD results are consistent with the XPS results. The linear relationship for the carbonyl

DOI: 10.1021/acscatal.5b00307
ACS Catal. 2015, 5, 3600−3608

group could not be obtained because the maximum temperature for TPD analysis on our equipment could only reach as high as 900 °C. The carbonyl group (m/z = 28 signal), which is considered as the active sites for the ODH reactions,[1,2,36] could not be completely desorbed at this temperature. It would make great sense only when the carbonyl group could be accurately quantified for the ODH reactions. Therefore, the oxygenated groups were not accurately quantified from the TPD profiles, and peak area was employed to preliminarily describe the number.

The above results from different characterizations demonstrate that the surface of the CNTs was efficiently functionalized with a large number of oxygenated groups after the HNO_3 treatment, while the ordered graphitic structure of the CNTs was not obviously destroyed.

3.2. Mass Titration. Mass titration is an effective tool to determine the Point of Zero Charge (PZC) of these CNTs samples.[28] The PZC of these CNTs was studied by two kinds of mass titration methods (the details for the titration are given in the Experimental Section). As shown in Figure 4, the PZC

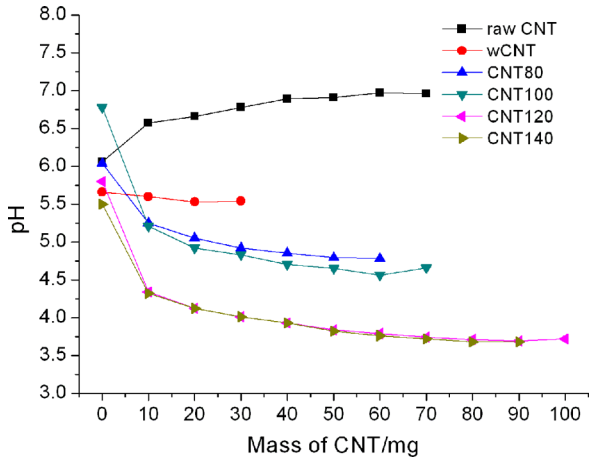

Figure 4. Determining the PZC of CNTs samples by mass titration method 1.

obtained from method 1 severely decreases to 3−4 after the CNTs are refluxed in HNO_3 at 120 or 140 °C, and the PZC of these CNTs samples decreases in the order of as-received CNT > wCNT > CNT80 > CNT100 > CNT120 ~ CNT140.

The results from mass titration method 2 are given in Figure 5, which is similar to that from Figure 4. The PZC of these CNTs also decreases in the order of as-received CNT > wCNT > CNT80 > CNT100 > CNT120 ~ CNT140. These results indicate that many acidic functional groups were generated during the HNO_3 treatment. Although the overall properties of oxygenated groups on the nanocarbons could be studied by PZC, the specific oxygen functional groups could not be identified and quantified.

3.3. Boehm Titration. Boehm titration is an effective tool to identify and quantify the specific oxygenated groups, especially for the carboxylic acid, lactone, phenol, and carbonyl groups,[29,30] using different bases with different basicity. Although the carbonyl group is sometimes regarded as a Lewis base group due to high electron density,[31] it could be titrated by the strong base $NaOC_2H_5$ in Boehm titration. Herein, the number of $NaHCO_3$ and Na_2CO_3 molecules adsorbed on the wCNT can be neglected, which further confirms that the adsorbed HCl or HNO_3 in the pretreatment

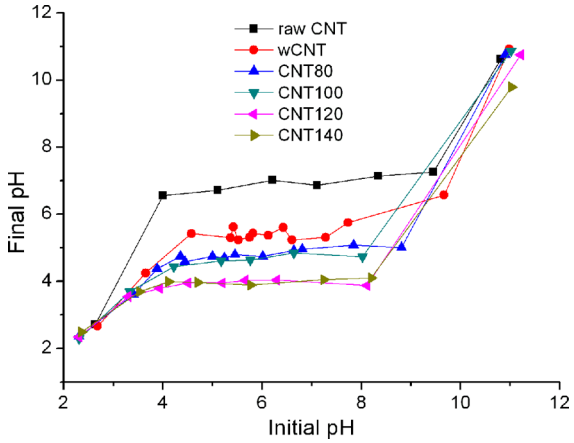

Figure 5. Determining the PZC of CNTs samples by mass titration method 2.

process could be almost removed during the washing step by distilled water before they went to the titration steps. As shown in Table 2, the number of all the four groups on the CNTs increases with the treating temperatures. These results are correlated with the results from XPS characterization, and a good linear relationship is found between the result of Boehm titration and XPS for the quantification of carbonyl group (Figure 6a). A linear relationship between the result of Boehm titration and XPS for the quantification of phenolic group is also found (Figure 6b), indicating that the result from Boehm titration and XPS characterization are convincible, at least for the carbonyl and phenol groups. Four different kinds of groups (carboxylic acid, anhydride, lactone, and ester groups) are contained in the O═C−O species from XPS characterization.[36] Among the four oxygenated groups, only carboxylic acid and lactone groups could be quantified by Boehm titration, and thus, the quantification for the O═C−O species from Boehm titration and XPS characterization could not be well correlated with each other (Figure S10). Compared to XPS characterization, Boehm titration has an obvious advantage to quantify the specific oxygen groups, because it is nearly impossible to completely deconvolute the XPS spectra into many individual peaks which represent the specific oxygenated groups.[31,36,43,44]

As mentioned above, the results from Boehm titration are consistent with the results from XPS analysis, and thus, the XPS results can be calibrated by the Boehm titration for our CNTs samples. As most of the oxygenated groups exist in the outer surface of the CNTs, the result from Boehm titration describes the surface properties of these CNTs, which is in accordance with that from XPS. In the Boehm titration, the relative error (δ) can be calculated in the following equation:

$$\delta = \Delta/L \times 100\%$$

Δ is the absolute error, while L is the true value. A larger true value corresponds with a smaller relative error. It is quite challenging to improve the accuracy of Boehm titration. In order to solve this problem, a large number of samples and a low base concentration should be used to enlarge the difference between samples and then reduce the titration error. From the results, it is found that the consumed base decreased in the order of $NaOC_2H_5$ > NaOH > Na_2CO_3, and thus, the relative error of the consumed base increases in the order of $NaOC_2H_5$ < NaOH < Na_2CO_3. In Boehm titration, the number of various

DOI: 10.1021/acscatal.5b00307
ACS Catal. 2015, 5, 3600−3608

Table 2. Surface Oxygenated Groups by Boehm Titration

	carboxylic acid		lactone		phenol		carbonyl	
sample	(μmol/m^2)	(mmol/g)	(μmol/m^2)	(mmol/g)	(μmol/m^2)	(mmol/g)	(μmol/m^2)	(mmol/g)
wCNT	0	0	0	0	0.47	0.11	0.20	0.05
CNT80	0.35	0.08	0.16	0.04	0.79	0.18	0.51	0.12
CNT100	0.50	0.12	0.16	0.04	1.04	0.24	0.86	0.20
CNT120	1.39	0.35	0.46	0.11	1.46	0.36	1.44	0.36
CNT140	1.50	0.41	0.48	0.13	1.4	0.39	1.47	0.41

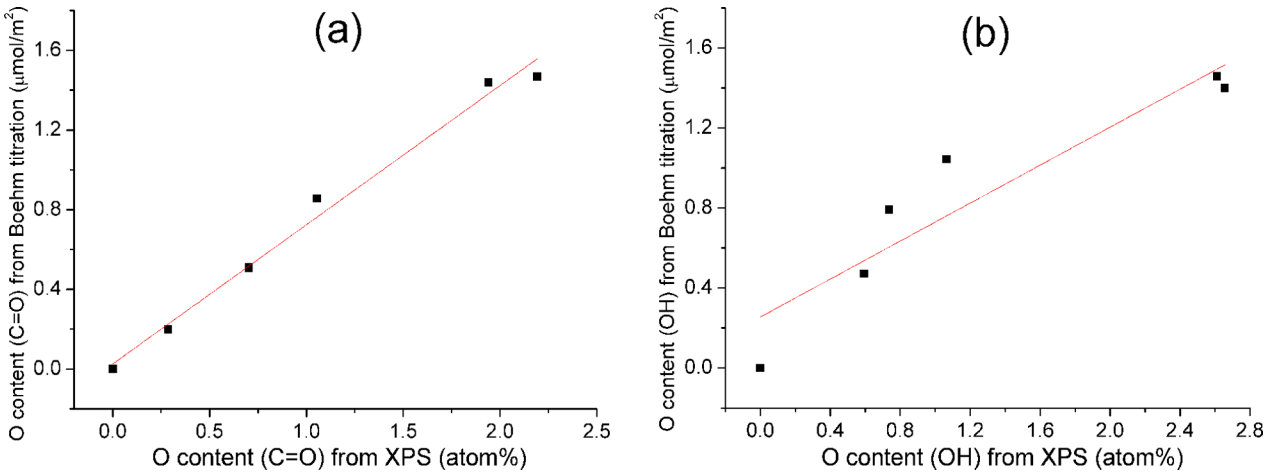

Figure 6. Correlate the O content for carbonyl group (a) and phenolic group (b) from Boehm titration with the surface atom content of O in carbonyl group and phenolic group from XPS analysis, respectively.

types of acidic groups was calculated under the assumption that C_2H_5ONa neutralized carboxylic acid, lactone, phenol, and carbonyl groups; NaOH neutralized carboxylic acid, lactone, and phenol groups; Na_2CO_3 neutralized carboxylic acid and lactone groups.[29,30] On the basis of this assumption, the number of carbonyl groups was calculated by the difference between the consumed $NaOC_2H_5$ and NaOH, whereas the number of phenolic groups was calculated from the difference between the consumed NaOH and Na_2CO_3. Therefore, the number of carbonyl groups was more accurate.

3.4. Acidity Characterizations by NH_3 Pulse Adsorption, NH_3-TPD, and FT-IR. In order to better understand the acidity of the nanocarbon catalysts, NH_3 pulse adsorption, NH_3-TPD, and FT-IR, which are widely applied to describe the acidity of solid acid, were employed to characterize the acidity. As shown in Table 3, the number of acidic sites calculated from

Table 3. Number of Acidic Sites Calculated from NH_3 Pulse Adsorption and Boehm Titration

sample	NH_3 pulse adsorption (μmol/m^2)	Boehm titration (μmol/m^2)
wCNT	0.31	0.47
CNT80	1.11	1.30
CNT100	1.57	1.71
CNT120	3.14	3.31
CNT140	3.29	3.39

NH_3 pulse adsorption is consistent with that obtained from Boehm titration. Herein, the number of acidic sites from Boehm titration is based on the number of relative strong acidic sites, including carboxylic acid, lactone, and phenol. The NH_3-TPD profiles are given in Figure 7. It can be seen that the NH_3 uptake increases with increasing treatment temperature for CNTs samples, and the main NH_3 release peak appears at

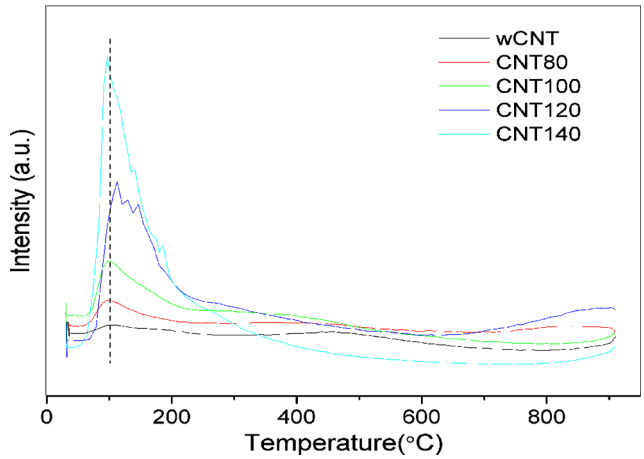

Figure 7. NH_3-TPD profiles of CNTs samples.

about 100 °C, indicating that most of the NH_3 molecules are weakly adsorbed. FT-IR analysis is performed to study the type and strength of acidic sites (Figure S11). When the sample preadsorbed with probe molecules (NH_3 and pyridine) was evacuated at room temperature, the signals for the adsorbed base molecules were not detected, indicating the acidity of the CNTs sample was very weak. Therefore, the adsorption of NH_3 found in NH_3 pulse adsorption experiment is likely ascribed to the weak interactions such as hydrogen bonds.[45]

3.5. Catalytic Activity of CNTs. The ODH of ethylbenzene is selected as a model reaction to study the roles of specific oxygenated groups. For the kinetic study, the conversions were controlled to less than 10%. The reactions were carried out at 245 °C, and it can be found from TG analysis that the ordered graphitic structure of CNTs was not

DOI: 10.1021/acscatal.5b00307
ACS Catal. 2015, 5, 3600−3608

obviously destroyed by O_2 at such low temperature. Negligible ethylbenzene conversion and styrene formation were observed in the blank experiment in the absence of catalysts, indicating that the ethylbenzene conversion and styrene formation were mainly result from the CNTs samples. The activities of these CNTs samples were compared with the activity of V/MgO catalyst, which was widely studied in ethylbenzene oxidative dehydrogenation during the past 20 years.[31,46,47] However, the 20 wt % V_2O_5/MgO catalyst was quickly deactivated, and the conversion decreased to only 0.5% after 20 h (Figure S12), which was much lower than that on CNTs catalysts—the conversion on the CNT140 could reach as high as 3.4% under the same conditions (Figure S13). The optimum reaction condition for V/MgO catalyst is at 500−600 °C in the presence of steam, whereas the catalyst could not give the best performance at such low temperature as low as 245 °C in the absence of steam. Steam is generally introduced into the reaction system catalyzed by V/MgO catalysts to suppress the undesired carbon deposition.

As reported previously, the carbonyl group is the active site for the ODH reactions,[1,2,31,32] and the reaction mechanism is assumed to be similar to that on transition metal oxide catalysts.[48] We correlated the ODH activity (initial styrene formation rate) with the surface number of carbonyl groups (Figure 8). It is found that the activity exhibits a linear

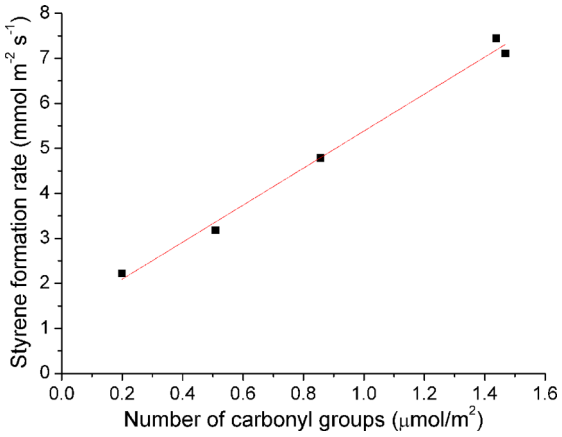

Figure 8. ODH activities (initial styrene formation rate) of CNTs samples with different surface number of carbonyl groups. Reaction conditions: 245 °C, 2.8 kPa ethylbenzene, 5.3 kPa O_2, He as balance, 100 mg of catalyst.

dependence on the number of carbonyl groups, further confirming that carbonyl groups are the active sites. These results indicate that the acid properties can indeed be successfully applied to identify and quantify the active sites in the ODH reactions. As shown in Figure 8, when the number of carbonyl groups is extrapolated to zero, the activity intersects the *y* axis at a nonzero value, which might be ascribed to the in situ formed ketonic carbonyl group on the defects.[36] The slope of the line represents the catalytic activity of single carbonyl group, namely the value of the TOF for these CNTs samples normalized by the number of active sites, which reflects the intrinsic activity of the nanocarbon catalysts. The value of TOF is 3.2×10^{-4} s^{-1}, which is very similar to our previous reported result under similar reaction conditions.[36] It seemed from early research that the ODH reactions occurred on the adjacent diketone groups,[31,32] and the TOF obtained was mainly ascribed to these adjacent diketone groups. Recently, it has been shown by our group that the isolated ketone group could also activate the dehydrogenation of C−H bond during the ODH reactions,[49] which demonstrates that the ODH reactions might occur both on the isolated ketone and the adjacent diketone groups, and the TOF obtained is likely to be the average value of these different types of ketone groups.

In our experiment, it was found that the activity of these CNTs slowly decreased with time on stream and stabilized at about 20 h. The long-term stability of the CNTs was also investigated, and it was found that the catalytic performance of the CNTs was very stable up to 112 h at 573 K (Figure S14). As shown in the high-resolution TEM images, the morphology of these spent CNTs slightly changes (Figure S15). The surface area of the CNT140 after reaction for 112 h decreased from 276 m^2/g to 240 m^2/g, while the pore volume slightly decreased from 1.41 cm^3/g to 1.21 cm^3/g. However, it can be found from the TG curves (Figure S16) that the initial temperature of the spent CNTs sample is much higher than that of the fresh sample, indicating the change in surface area and pore volume is likely attributed to the remove of intrinsic amorphous carbon instead of the carbon deposited during the reaction. Moreover, the carbon balance during the whole reaction remained stable around 100%, indicating the carbon deposition on the CNTs sample did not obviously occur. The surface oxygenated groups correspondingly changed when the activity was stabilized as we found from the XPS characterization (Table S1). However, the stabilized activities of these CNTs samples still show a linear dependence on the surface number of carbonyl groups (Figure S17).

The effect of O_2 partial pressure on the catalytic performance was studied, and the results are given in Figure 9. Here, the

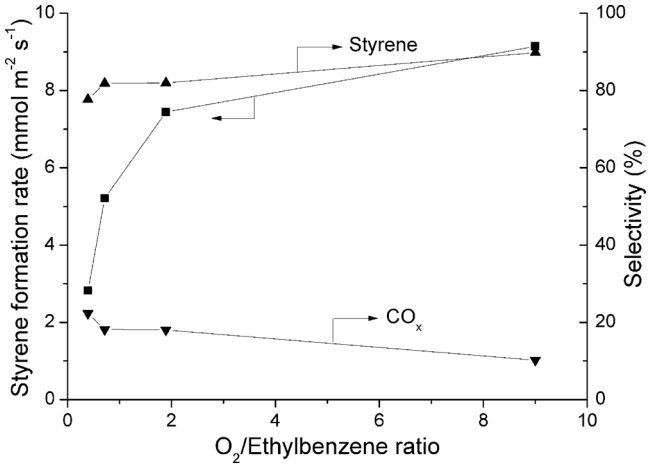

Figure 9. Effect of O_2/ethylbenzene partial pressure ratio on the catalytic performance. Reaction conditions: 245 °C, 2.8 kPa ethylbenzene, He as balance, 100 mg of catalyst.

partial pressure of ethylbenzene was fixed at 2.8 kPa. It can be found that the styrene formation rate increases significantly when the O_2/ethylbenzene partial pressure ratio increases from 0.4 to 1.9, and then the formation rate slowly increases with the further increase of O_2/ethylbenzene ratio. The dependence can be fitted using a reaction order of 0.34 in P_{O_2} (Figure S18), which is very similar to that in our previous report.[50] It can be also seen from Figure 9 that the styrene selectivity gradually increases when the ratio increases, while the CO_x selectivity

DOI: 10.1021/acscatal.5b00307
ACS Catal. 2015, 5, 3600−3608

correspondingly decreases. It seems that high O_2 pressure is favorable for the styrene formation.

The apparent activation energy from the ODH reaction rates at different temperatures from 245 to 300 °C for different CNTs samples was also studied (Figure S19). The activation energy of wCNT and CNT120 is around 61 and 60 kJ/mol, respectively, which further confirms that the active sites on the two CNTs samples are identical.

For better studying the acidity of nanocarbon, these CNTs samples were applied in two typical acid-catalyzed reactions, including Beckmann rearrangement and ring opening. The Beckmann rearrangement of cyclohexanone oxime is an important catalytic process because caprolactam, the main product of the reaction, is a precursor of Nylon-66, which is very important in industry. As expected, the conversion of cyclohexanone oxime exhibits a linear dependence on the number of acidic sites (Figure S20). Although the acidity of CNTs samples is weak, the maximum conversion can reach 44.2%, which is comparable to other solid acid catalysts such as HZSM-5, HY, and heteropoly acids under similar reaction conditions,[51] indicating the reaction proceeds well on weak acidic sites.

The ring opening of styrene oxide with methanol was also conducted to describe the acidity of these CNTs samples. It can be seen from Figure S21 that there is a linear relationship between the conversion of styrene oxide and the number of surface acidic sites. However, the maximum conversion is only 12.7%, which is too low compared to other acid catalysts.[52]

4. CONCLUSION

The acid properties of CNTs were thoroughly studied in this work. The surface of CNTs was efficiently functionalized with oxygenated groups, while the ordered graphitic structure was not obviously destroyed after refluxed in HNO_3 at different temperatures from 80 to 140 °C. The Point of Zero Charge, which reflected the overall acid properties of oxygenated groups, decreased in the following order of as-received CNT > wCNT > CNT80 ~ CNT100 > CNT120 ~ CNT140. Specific oxygenated groups, including carboxylic acid, lactone, phenol, and carbonyl groups, could be identified and quantified by Boehm titration, and the result was consistent with that from XPS characterization. For comparison, the acidity of these CNTs samples was also studied by NH_3 pulse adsorption, NH_3-TPD, and FT-IR, which are widely used to analyze the acidity of solid acid catalysts. The number of acidic sites from NH_3 pulse adsorption was consistent with that from Boehm titration; however, the strength of the acidic sites was very weak.

The ODH activity (initial styrene formation rate) exhibited a good linear dependence on the surface number of carbonyl groups, further confirming that carbonyl groups were the active sites in the ODH reactions. The TOF for all these CNTs samples was 3.2×10^{-4} s^{-1}, which reflected the intrinsic activity of the nanocarbon materials. Similar apparent activation energy (about 60 kJ/mol) was obtained on wCNT and CNT120, which further confirmed that the active sites on the two CNTs samples were identical. These CNTs samples were also applied in two typical acid-catalyzed reactions (Beckmann rearrangement and ring opening) to better understand their acidity, and a good linear relationship was found between the conversion and number of acidic sites.

■ ASSOCIATED CONTENT

Supporting Information

The Supporting Information is available free of charge on the ACS Publications website at DOI: 10.1021/acscatal.5b00307.

Supporting table and figures (PDF)

■ AUTHOR INFORMATION

Corresponding Author

*E-mail: dssu@imr.ac.cn. Tel.: +86 24 23971577. Fax: +86 83970019.

Notes

The authors declare no competing financial interest.

■ ACKNOWLEDGMENTS

The authors thank Xiaoying Sun and Bo Li (Institute of Metal Research, Chinese Academy of Sciences) for fruitful discussions. The authors also thank Feifei Xu (Dalian Institute of Chemical Physics, Chinese Academy of Sciences) for FT-IR analysis. Financial support is provided by Ministry of Science and Technology of China (2011CBA00504), the National Science Foundation of China (21133010, 51221264, 21261160487, 21411130120, 21473223), the "Strategic Priority Research Program" of the Chinese Academy of Sciences (XDA09030103), and the Doctoral Starting up Foundation of Liaoning Province, China (20121068).

■ REFERENCES

(1) Su, D. S.; Perathoner, S.; Centi, G. *Chem. Rev.* **2013**, *113*, 5782−5816.
(2) Su, D. S.; Zhang, J.; Frank, B.; Thomas, A.; Wang, X. C.; Paraknowitsch, J.; Schlögl, R. *ChemSusChem* **2010**, *3*, 169−180.
(3) Liang, C. D.; Xie, H.; Schwartz, V.; Howe, J.; Dai, S.; Overbury, S. H. *J. Am. Chem. Soc.* **2009**, *131*, 7735−7741.
(4) Liu, L.; Deng, Q. F.; Agula, B.; Zhao, X.; Ren, T. Z.; Yuan, Z. Y. *Chem. Commun.* **2011**, *47*, 8334−8336.
(5) Dreyer, D. R.; Jia, H. P.; Bielawski, C. W. *Angew. Chem., Int. Ed.* **2010**, *49*, 6813−6816.
(6) Kuang, Y. B.; Islam, N. M.; Nabae, Y.; Hayakawa, T.; Kakimoto, M. *Angew. Chem., Int. Ed.* **2010**, *49*, 436−440.
(7) Gao, Y. J.; Ma, D.; Wang, C. L.; Guan, J.; Bao, X. H. *Chem. Commun.* **2011**, *47*, 2432−2434.
(8) Chen, P. R.; Chew, L. M.; Kostka, A.; Xie, K. P.; Muhler, M.; Xia, W. *J. Energy Chem.* **2013**, *22*, 312−320.
(9) Yu, H.; Peng, F.; Tan, J.; Hu, X. W.; Wang, H. J.; Yang, J.; Zheng, W. X. *Angew. Chem., Int. Ed.* **2011**, *50*, 3978−3982.
(10) Yang, X. X.; Wang, H. J.; Li, J.; Zheng, W. X.; Xiang, R.; Tang, Z. K.; Yu, H.; Peng, F. *Chem. - Eur. J.* **2013**, *19*, 9818−9824.
(11) Su, F. Z.; Mathew, S. C.; Lipner, G.; Fu, X. Z.; Antoniett, M.; Blechert, S.; Wang, X. C. *J. Am. Chem. Soc.* **2010**, *132*, 16299−16301.
(12) Wang, D. W.; Su, D. S. *Energy Environ. Sci.* **2014**, *7*, 576−591.
(13) Pan, X. L.; Bao, X. H. *Acc. Chem. Res.* **2011**, *44*, 553−562.
(14) Dreyer, D. R.; Park, S.; Bielawski, C. W.; Ruoff, R. S. *Chem. Soc. Rev.* **2010**, *39*, 228−240.
(15) Muthuswamy, N.; Gomez, J.; Ochal, P.; Giri, R.; Raaen, S.; Sunde, S.; Rønning, M.; Chen, D. *Phys. Chem. Chem. Phys.* **2013**, *15*, 3803−3813.
(16) Xie, H.; Wu, Z. L.; Overbury, S. H.; Liang, C. D.; Schwartz, V. *J. Catal.* **2009**, *267*, 158−166.
(17) Schwartz, V.; Overbury, S. H.; Liang, C. D. In *Novel Materials for Catalysis and Fuels Processing*; Bravo-Suárez, J. J., Kidder, M. K., Schwartz, V., Eds.; American Chemical Society: Washington, DC, 2013; Vol. *1132*, pp 247−258.
(18) Wu, S. C.; Wen, G. D.; Liu, X. M.; Zhong, B. W.; Su, D. S. *ChemCatChem* **2014**, *6*, 1558−1561.

DOI: 10.1021/acscatal.5b00307
ACS Catal. 2015, 5, 3600−3608

(19) Su, C. L.; Acik, M.; Takai, K.; Lu, J.; Hao, S. J.; Zheng, Y.; Wu, P. P.; Bao, Q. L.; Enoki, T.; Chabal, Y. J.; Loh, K. P. *Nat. Commun.* **2012**, *3*, 1298.
(20) Abdullahi, I.; Davis, T. J.; Yun, D. M.; Herrera, J. E. *Appl. Catal., A* **2014**, *469*, 8−17.
(21) Qui, N. V.; Scholz, P.; Keller, T. F.; Pollok, K.; Ondruschka, B. *Chem. Eng. Technol.* **2013**, *36*, 300−306.
(22) Wu, S. C.; Wen, G. D.; Zhong, B. W.; Zhang, B. S.; Gu, X. M.; Wang, N.; Su, D. S. *Chin. J. Catal.* **2014**, *35*, 914−921.
(23) Sun, X. Y.; Wang, R.; Su, D. S. *Chin. J. Catal.* **2013**, *34*, 508−523.
(24) Ma, H. J.; Yang, X. M.; Wen, G. D.; Tian, G.; Wang, L.; Xu, Y. P.; Wang, B. C.; Tian, Z. J.; Lin, L. W. *Catal. Lett.* **2007**, *116*, 149−154.
(25) Tao, L. Z.; Yan, B.; Liang, Y.; Xu, B. Q. *Green Chem.* **2013**, *15*, 696−705.
(26) Hao, X.; Barnes, S.; Regalbuto, J. R. *J. Catal.* **2011**, *279*, 48−65.
(27) Lambert, S.; Job, N.; D'Souza, L.; Pereira, M. F. R.; Pirard, R.; Heinrichs, B.; Figueiredo, J. L.; Pirard, J. P.; Regalbuto, J. R. *J. Catal.* **2009**, *261*, 23−33.
(28) Lee, S. C.; Zhang, Z. T.; Wang, X. M.; Pfefferle, L. D.; Haller, G. L. *Catal. Today* **2011**, *164*, 68−73.
(29) Boehm, H. P.; Diehl, E.; Heck, W.; Sappok, R. *Angew. Chem., Int. Ed.* **1964**, *3*, 669−677.
(30) Boehm, H. P. *Carbon* **2002**, *40*, 145−149.
(31) Zhang, J.; Liu, X.; Blume, R.; Zhang, A. H.; Schlögl, R.; Su, D. S. *Science* **2008**, *322*, 73−77.
(32) Dathar, G. K. P.; Tsai, Y. T.; Gierszal, K.; Xu, Y.; Liang, C. D.; Rondinone, A. J.; Overbury, S. H.; Schwartz, V. *ChemSusChem* **2014**, *7*, 483−491.
(33) Pereira, M. F. R.; Órfão, J. J. M.; Figueiredo, J. L. *Appl. Catal., A* **1999**, *184*, 153−160.
(34) Zarubina, V.; Talebi, H.; Nederlof, C.; Kapteijn, F.; Makkee, M.; Melián-Cabrera, I. *Carbon* **2014**, *77*, 329−340.
(35) Figueiredo, J. L.; Pereira, M. F. R.; Freitas, M. M. A.; Órfão, J. J. M. *Ind. Eng. Chem. Res.* **2007**, *46*, 4110−4115.
(36) Qi, W.; Liu, W.; Zhang, B. S.; Gu, X. M.; Guo, X. L.; Su, D. S. *Angew. Chem., Int. Ed.* **2013**, *52*, 14224−14228.
(37) Edwards, E. R.; Antunes, E. F.; Botelho, E. C.; Baldan, M. R.; Corat, E. J. *Appl. Surf. Sci.* **2011**, *258*, 641−648.
(38) Bower, C.; Kleinhammes, A.; Wu, Y.; Zhou, O. *Chem. Phys. Lett.* **1998**, *288*, 481−486.
(39) Sadezky, A.; Muckenhuber, H.; Grothe, H.; Niessner, R.; Pöschl, U. *Carbon* **2005**, *43*, 1731−1742.
(40) Song, S. Q.; Yang, H. X.; Rao, R. C.; Liu, H. D.; Zhang, A. M. *Catal. Commun.* **2010**, *11*, 783−787.
(41) Rosenthal, D.; Ruta, M.; Schlögl, R.; Kiwi-Minsker, L. *Carbon* **2010**, *48*, 1835−1843.
(42) Frank, B.; Morassutto, M.; Schomäcker, R.; Schlögl, R.; Su, D. S. *ChemCatChem* **2010**, *2*, 644−648.
(43) Schwartz, V.; Xie, H.; Meyer, H. M., III; Overbury, S. H.; Liang, C. D. *Carbon* **2011**, *49*, 659−668.
(44) Abdullahi, I.; Davis, T. J.; Yun, D. M.; Herrera, J. E. *Appl. Catal., A* **2014**, *469*, 8−17.
(45) Li, C.; Zhao, A. Q.; Xia, W.; Liang, C. H.; Muhler, M. *J. Phys. Chem. C* **2012**, *116*, 20930−20936.
(46) Geisler, S.; Vauthey, I.; Farusseng, D.; Zanthoff, H.; Muhler, M. *Catal. Today* **2003**, *81*, 413−424.
(47) Oganowski, W.; Hanuza, J.; Kepiński, L. *Appl. Catal., A* **1998**, *171*, 145−154.
(48) Schraut, A.; Emig, G.; Hofmann, H. *J. Catal.* **1988**, *112*, 221−228.
(49) Sun, X. Y.; Li, B.; Su, D. S. *Chem. Commun.* **2014**, *50*, 11016−11019.
(50) Zhang, J.; Su, D. S.; Zhang, A. H.; Wang, D.; Schlögl, R.; Hébert, C. *Angew. Chem., Int. Ed.* **2007**, *46*, 7319−7323.
(51) Shiju, N. R.; Williams, H. M.; Brown, D. R. *Appl. Catal., B* **2009**, *90*, 451−457.
(52) Dhakshinamoorthy, A.; Alvaro, M.; Concepción, P.; Fornés, V.; Garcia, H. *Chem. Commun.* **2012**, *48*, 5443−5445.

DOI: 10.1021/acscatal.5b00307
ACS Catal. 2015, 5, 3600−3608